ISSN 1846-6168 (Print), ISSN 1848-5588 (Online)
https://doi.org/10.31803/tg-20231212075502

Original scientific paper
Received: 2023-12-12, Accepted: 2024-02-19

Assessing Adsorption and Desorption Performance in the Recovery of Volatile Organic Compounds: A Carbon Fiber Filter Design Perspective

Dong-Hwan Jeon, Hoon-Min Park, Hyun-Min Jung, Dal-Hwan Yoon*

Abstract: In this study, the activated carbon fiber filter design and VOC adsorption and desorption performance were evaluated based on the development of a filter regeneration device to treat VOCs in high efficiency and low cost. Activated carbon fiber (ACF) has the advantage of fast adsorption speed and high adsorption capacity because micropores are formed on the surface and a large specific surface area. However, the specific gravity is about 25 times lower than that of activated carbon (AC), so the amount of adsorbent that can fill the same volume is small. In order to solve this problem, the regeneration device is implemented by repeating adsorption and regeneration for a short time, and a cylindrical adsorption filter made of activated carbon fiber is designed according to the operating conditions of the regeneration device. At this time, the pollutant gas and regenerated air are uniformly distributed over the entire adsorbent, and the flow characteristics according to the supply of the pollutant gas and the regeneration gas are analyzed. When the size of the lower part of the cylindrical adsorption filter is smaller than the size of the upper part under the condition that the pollutant gas flows downward, a uniform distribution of the pollutant gas is possible. In addition, as the space velocity decreases, the adsorption capacity decreases, and the differential pressure increases rapidly. Through the regeneration experiment, it was confirmed that the desorption concentration of MEK was higher and the desorption concentration was higher. In addition, the regenerated air is uniformly dispersed throughout the adsorption filter, toluene, o-xylene, and methyl ethyl ketone, which are representative substances of volatile organic compounds (VOCs), are injected with 400 ppm, and then regenerated air is supplied at 150 °C to analyze adsorption characteristics and regeneration concentrations. As a result of the experiment, the adsorption capacity ratio to 1 g of regeneration air according to the type of VOCs was 0.48, 0.36, and 0.25 g in the order of o-xylene, toluene, and methyl ethyl ketone. In addition, as the space velocity decreases, the adsorption capacity decreases, and the differential pressure increases rapidly. Through the regeneration experiment, it was confirmed that the desorption concentration of MEK was higher and the desorption concentration of o-xylene was discharged at a relatively low concentration. Moreover, even if the adsorption concentration changes, there was no difference in the regeneration concentration change. Therefore, the filter was designed based on the spatial speed of the regeneration device of 51,000 -h or less, and the adsorption capacity ratio to 1 g of the regeneration air amount was 0.1 g, thereby enhancing the filter's recycling performance and VOCs emission effect.

Keywords: activated carbon fiber; adsorption; flow analysis; regeneration system; volatile organic compounds

1 INTRODUCTION

Efforts to reduce greenhouse gases are being made in various fields as global warming caused by greenhouse gases has reached a serious level worldwide. Volatile organic compounds (VOCs), known as representative greenhouse gases, can be efficiently and safely recovered and recycled at VOC emission sites, thereby minimizing environmental pollution and maximizing greenhouse gas reduction when generating desorption heat energy using renewable energy [1-10]. VOCs are selectively discharged from the discharge system through adsorption, oxidation, absorption, and condensation, depending on their material properties and concentration. Until now, most of the poorly soluble VOCs discharged below 800 ppm using activated carbon have been treated with adsorption technology. Activated carbon has been used for a long time for gas separation and purification because it has the advantage of having pore structures of various sizes. It has been used as an adsorbent for gas purification in a new field through chemical treatment [11].

Activated carbon fibers have developed micropores on the fiber surface, are capable of rapid adsorption due to their large specific surface area, and are known to have superior adsorption rate and selective gas adsorption than activated carbon [12, 13]. The activated carbon fiber can control a specific surface area through heat treatment and formation processes in the manufacturing process and is used for gas separation purification or water treatment in various fields [14-18]. However, since activated carbon fiber have a specific gravity of about 25 times lower than activated carbon, the same volume can be filled with adsorbents. Therefore, there is a problem that the adsorption efficiency is better than that of activated carbon, but the adsorption time needs to be longer. In order to solve this problem and utilize high-performance adsorption properties, adsorption and regeneration must be repeated for a short period.

In addition, the pressure drop characteristics for process gas and the airflow characteristics for the uniform distribution of process gas and regeneration gas throughout the filter should be considered [19, 20]. These characteristics are essential factors in device design, and pollutant gas purification characteristics may vary depending on the filter shape and structure [21]. Computational flow analysis can confirm the airflow characteristics and the optimal shape can be obtained [22, 23].

Table 1 Comparison of design specifications of activated carbon fiber and activated carbon adsorbent in VOCs treatment equipment.

Adsorbent type		Activated carbon fiber	Activated carbon
Adsorbent	Fill amount	56 kg × 2 = 112 kg	1400 kg × 2 = 2800 kg
	Layer thickness	120 mm	600 mm
Change time	Adsorption	6 min/col	120 min/col
	Escape	6 min/col	30 min/col
Adsorbent container	$L \times W \times H$	1600×1100×1500	2600×1500
	Volume	2.64 m^3	7.96 m^3
Recall consumption	Vapor	350 kg/h	1660 kg/h
	Cooling water	10 t/h	25 t, 48 t/h
	Power	15 kW	15 kW

Tab. 1 compares the design specifications of activated carbon fibers and activated carbon adsorbents in VOCs treatment units. In the case of activated carbon, it consists of a macro-pore with a pore diameter of 50 nm, a meso-pore with a pore diameter of 2-50 nm, and a micro-pore with a pore size of 2 nm or less deep inside. It is possible to adsorb various substances and is inexpensive, but the adsorption and desorption rate is slow and requires a lot of renewable energy. Activated carbon fibers mainly have micro-pores formed on the surface, so fast adsorption and desorption, less renewable energy is required, and the device can be miniaturized due to excellent adsorption efficiency. Therefore, when an activated carbon fiber adsorbent is used in comparing the performance of activated carbon and activated carbon fiber, the amount of desorption steam supplied is only 20% compared to activated carbon, the size of the device is 33%, the operating cost can be reduced by 4.8 times, and the size of the facility can be reduced.

In this study, activated carbon fibers are designed in the shape of a filter to develop a system to process VOCs with high efficiency and low cost, and a computational flow analysis and VOC adsorption and desorption characteristics were conducted to derive primary design conditions for adsorption filters.

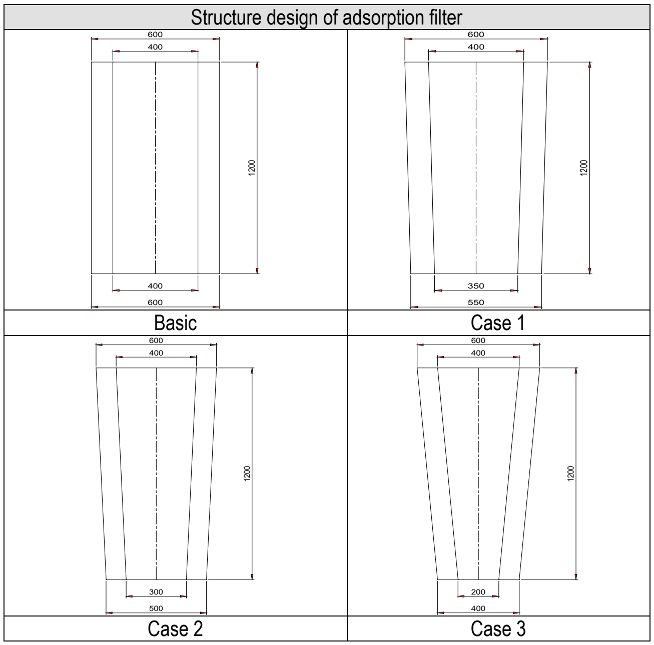

Figure 1 Adsorption filter design for flow analysis

2 IMPLEMENTATION OF OPTIMAL ACTIVATED CARBON FIBER FOR ADSORPTION

Using the high adsorption properties of ACF and designing a filter shape that can adsorb and regenerate quickly, the optimal fluid flow was confirmed using computational flow analysis. The program used for the flow analysis was Solid Edge 2022 Classic version. The adsorption filter shape is cylindrical, generally used in filters, and the grid size for the analysis area was 0.002 m. A matrix consisting of 24,934 cells was applied. The sagging gas supplied to the adsorption filter flows into the lower part of the filter, and the flow rate is 50 Nm^3/min. Recycled air flowed into the top of the adsorption filter and steam controls at a pressure of 2 bar. Gage was supplied at 0.83 kg/min.

Fig. 1 shows the basic filter size designs with an external diameter of 600 mm, an internal diameter of 400 mm, and a height of 1500 mm. In addition, the size of the lower filter was adjusted to 350 mm, 300 mm, and 200 mm to derive a shape in which pollution gas and regenerated air can be dispersed evenly throughout the adsorption filter.

Fig. 2 shows the flow analysis results under adsorption conditions according to the filter shape change. The basic configuration confirmed that gas flow concentrates at about 1 m/c at all eight corners. In addition, as the size of the lower part of the filter decreases, the concentration of the gas flow decreases, confirming of the gas flow decreases, confirming that the gas flow distributes throughout the filter.

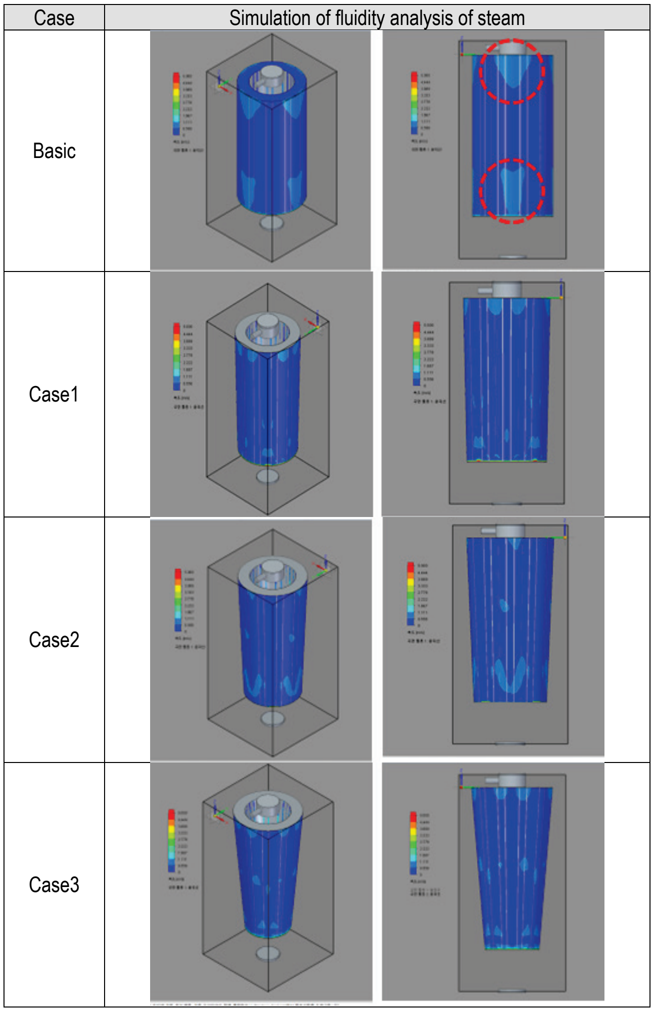

Figure 2 Results of confirmation of gas flow characteristics under adsorption conditions

Fig. 3 shows the results of flow analysis under regeneration conditions. In the case of the Case 1 shape filter, steam is distributed relatively evenly than the primary filter, but it shows that strong steam flow is generated locally at the bottom. In the case of Case 2 shape filters, steam is distributed and supplied to the entire filter compared to Case 1. However, steam flow concentrates around the corner of the upper chamber of the filter, and it shows that there are areas where steam is not supplied intermittently to the middle and lower ends of the filter. The Case 3 shape filter also shows the supplied steam concentration under the filter, but the steam is evenly distributed and supplied compared to the primary Case 1 and 2 shape filters. Therefore, it judges that the Case 3-shaped filter is the most efficient for regenerating the adsorption filter using a steam supply.

Case	Simulation of fluidity analysis of steam
Basic	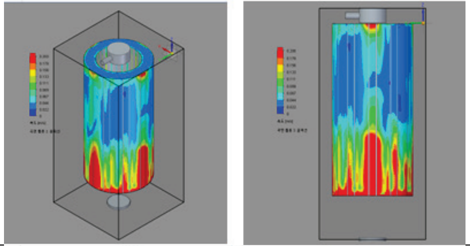
Case1	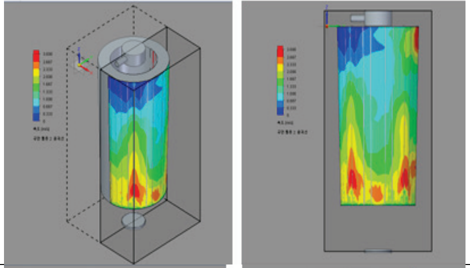
Case2	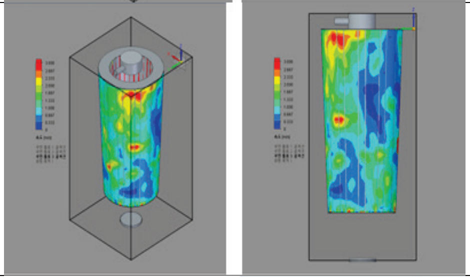
Case3	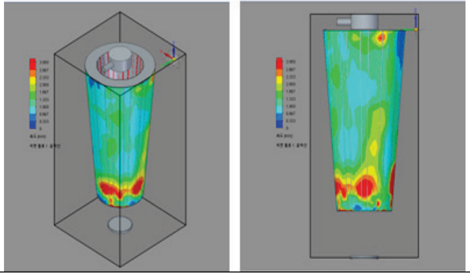

Figure 3 Results of confirmation of gas flow characteristics under desorption conditions

Fig. 4 designs and manufactures a wrinkle filter using activated carbon fiber, which is a filter adsorption material, based on the gas flow analysis in Fig. 3. A wrinkle pattern is designed in consideration of a 5 CMM-class regenerator, and the adsorption filter has an outer diameter of 200 mm and an inner diameter of 100 mm. At this time, the wrinkle height is 30 mm and the number of wrinkles is 30. And after calculating the area required for the adsorbent according to the processing gas flow rate, the filter height is set to 500 mm by applying a margin of 10 %. During the filter manufacturing process, a SUS mesh is attached to support the wrinkle shape of the activated carbon fiber adsorbent.

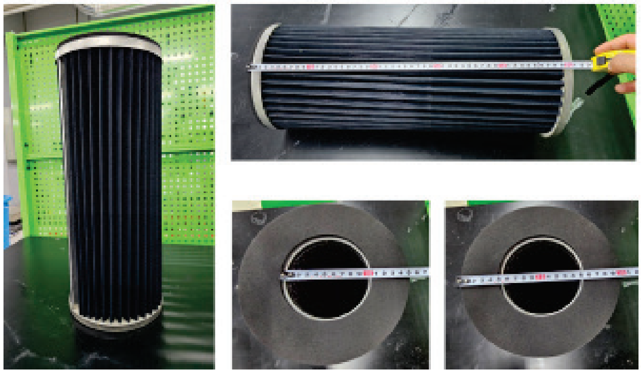

Figure 4 Wrinkle filter of 5 CMM grade

3 ADSORPTION CHARACTERISTICS OF VOCS IN ACTIVATED CARBON FIBER

Fig. 5 shows the configuration of the test device for checking the adsorption performance of activated carbon fibers. The activated carbon fiber used in this study was a product with a thickness of 3 mm and a specific surface area of 1,700 m^2/g sold by the Korea Active Carbon Fiber Company to recover organic solvents. The test gas supplies gas flow rate using a mass flow controller manufactured by Brooks. For the adsorption, Toluene, o-xylene, and methyl ethyl ketone reagents, which are representative materials of volatile organic compounds, were used. The vaporized liquid adsorbate in the test gas controls the desired concentration and is used in adsorption experiments. The liquid adsorbate vaporizer was controlled at 150 °C using a PID-type temperature controller after installing a heating wire on the outer surface of the cylindrical reactor. The liquid adsorbate uses a micro syringe to precisely supply the control at 2-12 mL/hr. After mixing the adsorbed material vaporized into a gaseous state with the test gas, the concentration of the adsorbed gas confirms the use of an FID-type portable THC analyzer manufactured by Polaris. The research conducts the adsorption experiment by converting the test gas to be supplied to the adsorption reactor using a valve once it confirms the test gas concentration.

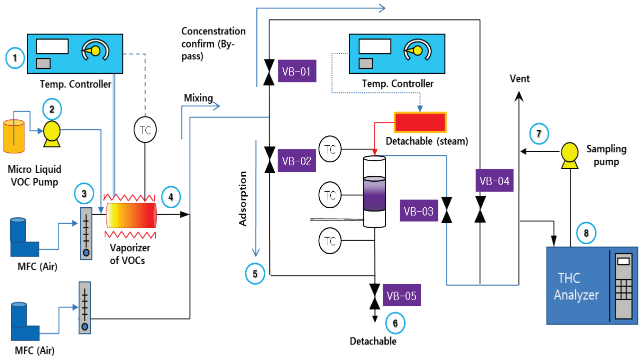

Figure 5 Configuration diagram of activated carbon fiber adsorption performance test

For the stable performance of the development facility and smooth operation, an integrated control system (Timer and Integrated Control System) operation method is proposed based on the adsorbent performance evaluation test results. This control method is a method in which each chamber operation is controlled by a timer, and the operation of another chamber is sequentially performed based on the operation state of the chamber in which adsorption is performed. The blower operation operates to maintain a constant discharge gas flow rate by varying and controlling the blower rotation speed according to the filter differential pressure. If the inverter proceeds in real time, a change in the discharge gas flow rate may occur temporarily due to an error in the measuring instrument or the influence of production facilities. Therefore, it is controlled with a sequential control program so that it is variably operated according to the difference between the average filter differential pressure value measured for 2 to 5 minutes and the standard differential pressure value. Fig. 6 shows a net self-control flowchart.

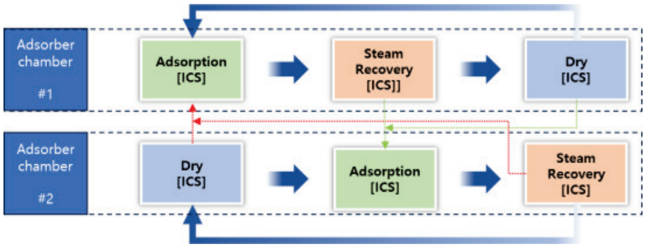

Figure 6 Net self-control flowchart

Tab. 2 shows the evaluation conditions for the adsorption performance of activated carbon fibers. The adsorption characteristics according to spatial speed change confirm the adsorption characteristics under spatial speed (10,000 ~254,000 m^3/hour) conditions by installing activated carbon fibers in the adsorption reactor and adjusting the adsorbent filling height in the range of 3 to 75 mm under the test gas supply flow rate of 100 L/min and VOCs concentration of 400 ppm.

Table 2 The adsorption and regeneration test conditions

Category		Contents
Column size		100 mm × 400 mm H
VOCs	Supply method	Micro syringe pump
	Adsorbate	Toluene, o-xylene, MEK
Test gas		Air (50, 100 L/min)
Operation Condition	Temperature/Concentration	26-28 °C/100-400 ppm
	Height of ACF	3, 6, 9, 15, 25, 75 mm

4 EXPERIMENTAL RESULTS

The adsorption characteristics according to spatial speed change confirm the adsorption characteristics under spatial speed conditions by installing activated carbon fibers in the adsorption reactor and adjusting the adsorbent filling height in the range from 3 to 75 mm under the test gas supply flow rate of 100 L/min and VOCs concentration of 400 ppm. As the spatial speed increased, the adsorption capacity for 1 g of regenerated air capacity tended to increase from 0.36 g to 0.40 g, but the adsorption capacity tended to decrease based on the breakthrough point. And the breakthrough time is maintained at 9 minutes and 15 seconds, likely to the operating time of commercial facilities at a spatial speed of 51,000 m^3/hour. Fig. 7 shows the adsorption characteristics and breakthrough time results according to the change in the conditions of Tab. 3.

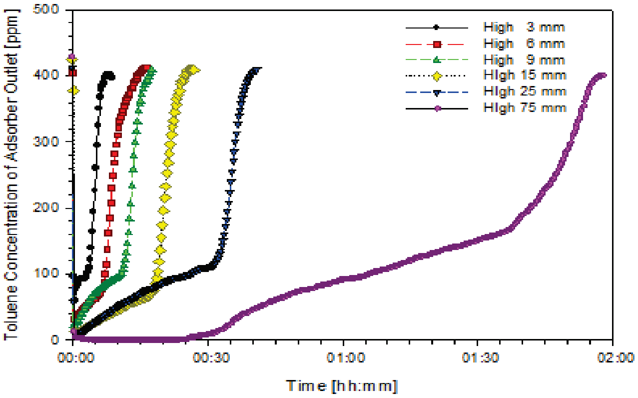

Figure 7 The toluene adsorption concentration of the adsorption outlet

Fig. 8 show the changes in the adsorption layer thickness and differential pressure with respect to the spatial velocity.

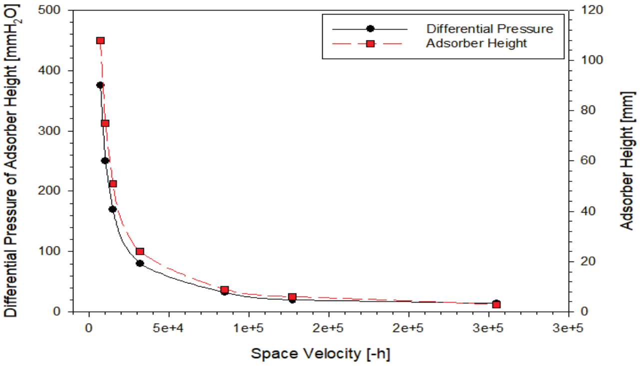

Figure 8 Variation of adsorption height and differential pressure with respect to spatial velocity

Table 3 Comparison of the space velocity and the differential pressure characteristics in the adsorption thickness

Adsorption thickness (mm)	Space velocity (SV) (m^3/hour)	Differential pressure (mmH$_2$O)
24	32,000	80
9	85,000	32
6	127,000	20
3	254,000	14

Table 4 Variable adsorption performance according to concentration change

Concentration (ppm)	Adsorption weight (g)	Total adsorption (g)	Adsorption quantity (g/g)	THC 100 ppm (g)	Effective adsorption (42 ppm)
200	40.37	13.55	0.34	0.14	71' 15"
300	40.37	14.18	0.35	0.14	46' 45"
400	40.37	14.37	0.36	0.14	34' 30"

Tab. 3 presents the comparison results of space velocity and differential pressure characteristics according to the adsorption height and the adsorption thicknesses 3, 6, 9 and 24 mm of the activated carbon filter. When the adsorption thickness decreases, the space velocity increases, while the differential pressure decreases.

Tab. 4 confirms the variable adsorption performance according to the change in concentration while supplying toluene concentration at 200, 300, and 400 ppm.

Fig. 9 show the ACF adsorption amount characteristics according to changes in the toluene concentration.

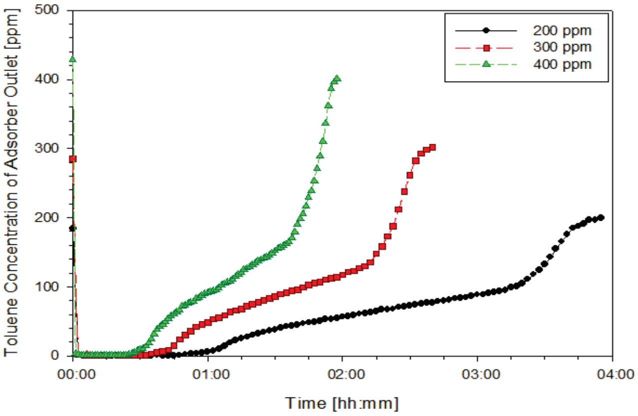

Figure 9 Adsorption curve according to changes in toluene concentration

Fig. 10 shows the desorption characteristics curve of the activated carbon filter according to the adsorption concentration. We can confirm the maximum desorption time.

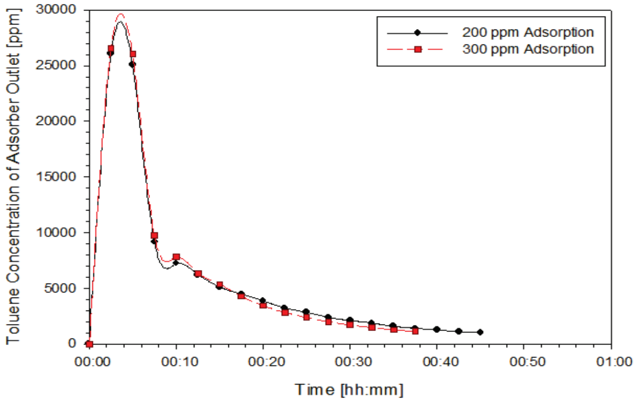

Figure 10 Desorption characteristics according to adsorption concentration

As the concentration of the adsorbed material increased, the amount of adsorption and the time required for the breakthrough point increased. However, the adsorption capacity for effective breakthrough point was 0.14 g/g. The difference between the total adsorption amount according to the concentration change and the adsorption capacity at the breakthrough point was not significant because adsorption from activated carbon fibers takes place on the surface of the adsorbent.

Tab. 5 is to estimate the experimental adsorption performance according to the Toluene, o-xylene, and MEK as representative materials to confirm the adsorption characteristic.

Fig. 11 compares the adsorption characteristics according to three gas types of VOCs. The adsorption characteristic experiment according to the change in the simulated gas of Toluene, the adsorption amount and the breakthrough time tended to be longer as the concentration increased, but the adsorption capacity up to the effective breakthrough time was the same at 0.14 g.

Table 5 Adsorption experiment data by volatile organic compounds type

Material	Adsorption weight (g)	Total adsorption (g)	Adsorption quantity (g/g)	THC 100 ppm (g)	Effective adsorption (42 ppm)
Toluene	40.37	14.37	0.36	0.14	34' 30"
O-xylene	40.37	19.21	0.48	0.19	41' 15"
MEK	40.37	10.05	0.25	0.09	29' 45"

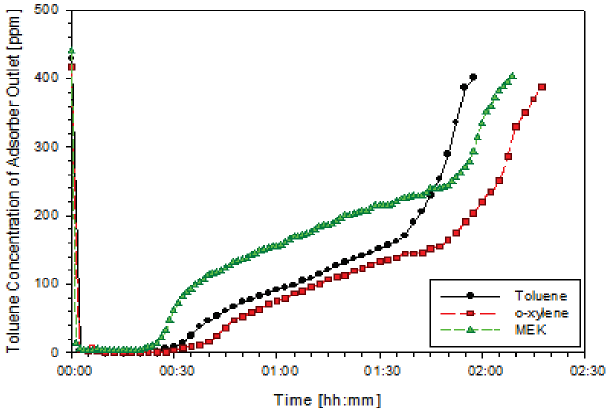

Figure 11 Adsorption curve according to adsorbate type

Fig. 12 confirms the regeneration characteristics according to the type of volatile organic compound and the maximum regeneration concentration of MEK, which has the lowest boiling temperature of the material, was the highest at 89,146 ppm, and desorption completes within about 5 minutes.

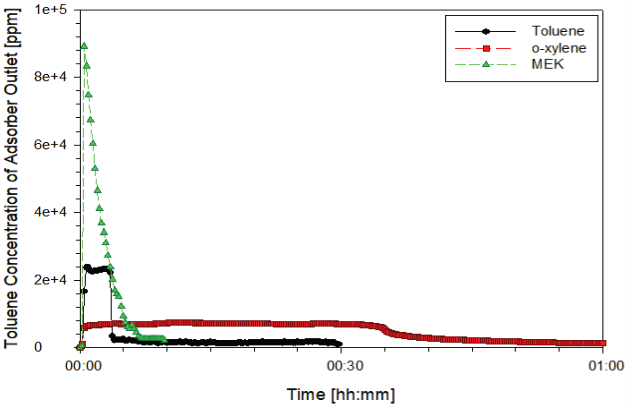

Figure 12 Desorption concentrations according to adsorbate type

On the other hand, o-xylene, with the highest boiling temperature, had the lowest desorption concentration of 7,528 ppm. After the desorption operation started, it was discharged at a specific concentration for about 35 minutes and gradually decreased. The desorption air temperature was 150 °C under the same conditions. However, it is necessary to maintain 30 °C higher than the adsorbent material's boiling temperature to complete the adsorbent's regeneration quickly.

Fig. 13 shows the adsorbent regeneration characteristics according to the change in the amount of dry air. When the amount of air increases by 1 L/min based on the amount of dry air 16.8 L/min, the adsorption efficiency increases by about 0.06 %, and when the amount of dry air is supplied at 42 L/min, the adsorption performance is maintained up to 96.4 % of the initial adsorption performance.

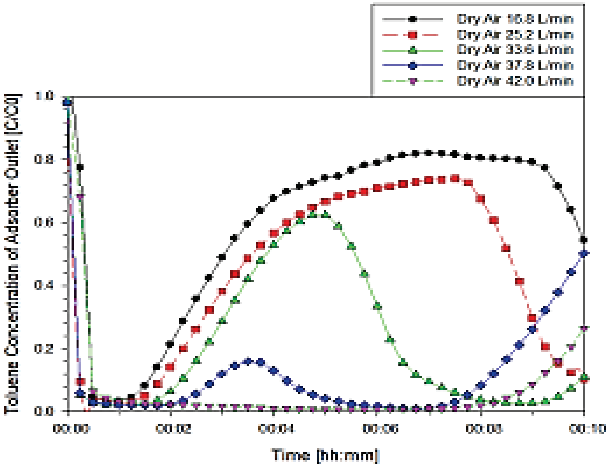

Figure 13 Regeneration characteristics according to the change in dry air amount

Fig. 14 compares the regeneration characteristics according to the supply location of dry air. When the amount of dry air was 42 L/min, the supply location of dry air was adjusted to the upper part of the reactor, the lower part of the reactor, and the lower part of the heat exchanger, and the regeneration characteristics were compared according to each condition.

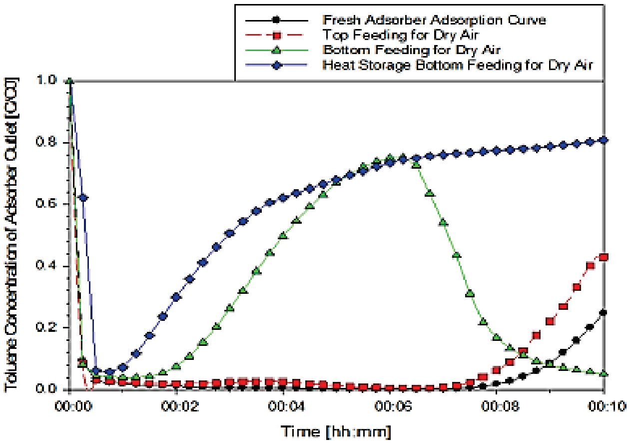

Figure 14 Comparison of the regenerative characteristics according to the supply location of dry air

When supplied to the upper part of the reactor, similar performance was shown at about 96.4 % of the initial adsorption performance. As a result of testing in the order of the lower part of the reactor and the lower part of the heat exchanger, the regeneration efficiency decreased by 69.8% and 42.2 %, respectively. When dry air is supplied to the lower part of the heat exchanger, it is judged that the drying performance decreases due to the residual moisture inside the heat exchanger, and the regeneration performance of the adsorbent decreases.

As a result of the hot air regeneration experiment, according to the adsorption concentration of Toluene, the maximum regeneration concentration was about 26,000 ppm and 64 % of the desorption after about 10 minutes of completion. The discharge time of 5,000 ppm or more, which can condense at low temperatures, was about 15 minutes, and continuous operation was determined if the adsorbent fills twice the total adsorption amount of the adsorbent for continuous operation facility application.

5 CONCLUSION

In this study, the flow characteristics according to the shape of the adsorption filter were checked to design an adsorption filter to efficiently process volatile organic compounds using activated carbon fibers, and a shape in which pollution gas can disperse evenly throughout the filter was derived. In addition, excellent adsorption efficiency and fast adsorption properties of activated carbon fibers confirm the adsorption and desorption experiments using Toluene, o-xylene, and methyl ethyl ketone. In order to use activated carbon fiber as an adsorption filter material, the adsorption and desorption time must be kept short, so it is necessary to control the regeneration air temperature 20 °C higher than the vaporization temperature of the adsorbent, and it is appropriate to maintain the acceptable adsorbent filling height above 32,000 m^3/hour. As a follow-up study, based on the design data obtained through the experiment, it plans to manufacture commercial facilities with a 100 Nm^3/min scale and link the production process. Once planned testing is complete, which expects the commercial facility to secure the design and operational technology.

Acknowledgments

This study was supported by the Tech-bridge project supported by the Small and Medium Business Technology Information Promotion Agency (business number RS-2022-00141809).

6 REFERENCES

[1] Borrego, C., Gomes, P., Barros, N. & Miranda, A. I. (2020). Importance of handling organic atmospheric pollutants for assessing air quality. *Journal of Chromatography A*, 889(1-2), 271-279. https://doi.org/10.1016/s0021-9673(00)00230-2

[2] Colbeck, I. & Mackenzie, A. R. (1994). *Air pollution by photochemical oxidants*. Elsevier, Amsterdam. https://doi.org/10.1016/0269-7491(95)90028-4

[3] Gray, H. A., Cass, G. R., Huntzicker, J. J., Heyerdahl, E. K. & Rau, J. A. (1986). Characteristics of atmospheric organic and elemental carbon particle concentrations in Los Angeles. *Environmental Science and Technology*, 20, 580-582. https://doi.org/10.1021/es00148a006

[4] Middlebrook, A. M., Murphy, D. M. & Thomson, D. S. (1998). Observations of organic material in individual marine particles

at Cape Grim during the first aerosol characterization experiment (ACE 1). *Journal of Geophysical Research*, 103, 16475-16483. https://doi.org/10.1029/97jd03719

[5] Grosjean, D. (1992). In situ organic aerosol formation during a smog episode: Estimated production and chemical functionality. *Atmospheric Environment*, 26A, 953-963. https://doi.org/10.1016/0960-1686(92)90027-i

[6] Hildemann, L. M. Rogge, W. F., Cass, G. R., Mazurek, M. A. & Simoneit, B. R. T. (1996). Contribution of primary aerosol emissions from vegetation-derived sources to fine particle concentrations in Los Angeles. *Journal of Geophysical Research*, 101, 19541-19549. https://doi.org/10.1029/95jd02136

[7] Schauer, J. J., Rogge, W. F., Hildemann, L. M., Mazurek, M. A., Cass, G. R. & Simoneit, B. R. T. (1996). Source apportionment of airborne particulate matter using organic compounds as tracers. *Atmospheric Environment, 30*(22), 3837-3855. https://doi.org/10.1016/1352-2310(96)00085-4

[8] Forstner, H. J. L., Flagan, R. C. & Seinfeld, J. H. (1997). Molecular speciation of secondary organic aerosol from photooxidation of the higher alkenes: 1-octene and 1-decene. *Atmospheric Environment, 31*(13), 1953-1964. https://doi.org/10.1016/s1352-2310(96)00356-1

[9] Odum, J. R., Jungkamp, T. P. W., Griffin, R. J., Flagan, R. C. & Seinfeld, J. H. (1997). The atmospheric aerosol-forming potential of whole gasoline vapour. *Science*, 226, 96-99. https://doi.org/10.1126/science.276.5309.96

[10] de P. Vasconcelos, L. A., Macias, E. S. & White, W. H. (1994). Aerosol composition as a function of haze and humidity levels in the southwestern US. *Atmospheric Environment*, 28, 3679-3691. https://doi.org/10.1016/1352-2310(94)00187-p

[11] Sircar, S., Golden, T. C. & Rao, M. B. (1996). Activated carbon for gas separation and storage. *Carbon*, 34(1), l-12. https://doi.org/10.1016/0008-6223(95)00128-x

[12] Brasquet, C. & Le Cloirec, P. (1997). Adsorption onto activated carbon fibers: Application to water and air treatments. *Carbon,* 35(9), 1307-1313. https://doi.org/10.1016/s0008-6223(97)00079-1

[13] Mangun, C. L., Yue, Z. R., Economy, J., Maloney, S., Kemme, P. & Cropek, D. (2001). Adsorption of organic contaminants from water using tailored ACFs. *Chem. Mater*., 13, 2356-2360. https://doi.org/10.1021/cm000880g

[14] Yue, Z. & Economy, J. (2016). Carbonization and activation for production of activated carbon fibers. Chen, J. Y. (Ed.), Activated carbon fiber and textiles. *Woodhead Publishing*, 61-139. https://doi.org/10.1016/b978-0-08-100660-3.00004-3

[15] Das, D., Gaur, V. & Verma, N. (2004). Removal of volatile organic compound by activated carbon fiber. *Carbon*, 42, 2949-2962. https://doi.org/10.1016/j.carbon.2004.07.008

[16] Fuertes, A. B., Marbán, G. & Nevskaia, D. M. (2003). Adsorption of volatile organic compounds by means of activated carbon fibre-based monoliths. *Carbon*, 41, 87-96. https://doi.org/10.1016/s0008-6223(02)00274-9

[17] Singh, K. P., Mohan, D., Tandon, G. S. & Gupta, G. S. D. (2002). Vapor-phase adsorption of hexane and benzene on activated carbon fabric cloth: Equilibria and rate studies. *Ind. Eng. Chem. Res.*, 41, 2480-2486. https://doi.org/10.1021/ie0105674

[18] Ramos, M. E., Bonelli, P. R., Cukierman, A. L., Ribeiro Carrott, M. M. L. & Carrott, P. J. M. (2010). Adsorption of volatile organic compounds onto activated carbon cloths derived from a novel regenerated cellulosic precursor. *Journal of Hazardous Materials*, 177(1-3), 175-182. https://doi.org/10.1016/j.jhazmat.2009.12.014

[19] Dabrowski, A. (2001). Adsorption from theory to practice. *Advances in Colloid and Interface Science*, 93, 135-224. https://doi.org/10.1016/s0001-8686(00)00082-8

[20] Payet, S., Boulaud, D., Madelaine, G. & Renoux, A. (1992). Penetration and pressure drop of a HEPA filter during loading with submicron liquid particles. *Journal of Aerosol Science, 23*(7), 723-735. https://doi.org/10.1016/0021-8502(92)90039-x

[21] Thomas, D., Contal, P., Renaudin, V., Penicot, P., Leclerc, D. & Vendel, J. (1999). Modelling pressure drop in HEPA filters during dynamic filtration. *Journal of Aerosol Science, 30*(2), 235-246. https://doi.org/10.1016/s0021-8502(98)00036-6

[22] Baléo, J. N., Subrenat, A. & Cloirec, P. L. (2000). Numerical simulation of flows in air treatment devices using activated carbon cloths filters. *Chemical Engineering Science, 55*(10), 1807-1816. https://doi.org/10.1016/s0009-2509(99)00441-8

[23] Kim, J. B. (2018). A Study of Heat Generation Materials using Carbon Fiber Silicon Coating Applying Big Data Analysis Technology. *International Journal of Advanced Science and Technology*, 119, 25-32. https://doi.org/10.14257/ijast.2018.119.03

Authors' contacts:

Dong-Hwan Jeon
Institute for Advanced Engineering,
175-28 Goan-ro 51beon-gil, Cheoin-gu, Yongin-si, Gyeonggi-do, Korea
jeon-76@iae.re.kr

Hoon-Min Park
EM SOLUTION Co. Ltd. Kyunggi-do, Suwon, Korea
Graduate School of Mechanical Engineering, Kyunggi University
hmpark@emsolutions.co.kr

Hyun-Min Jung
EM SOLUTION Co. Ltd. Kyunggi-do, Suwon, Korea
Graduate School of Mechanical Engineering, Kyunggi University
hmjung@emsolutions.co.kr

Dal-Hwan Yoon
(Corresponding author)
Department of Electronic Engineering, Semyung University,
65 Semyung-ro, Jecheon-si, Chungcheongbuk-do, 27136, Korea
yoondh@semyung.ac.kr